Journal of
Synchrotron
Radiation

ISSN 0909-0495

Received 8 February 2012
Accepted 28 July 2012

Diffraction-enhanced X-ray imaging under low-temperature conditions: non-destructive observations of clathrate gas hydrates

Satoshi Takeya,[a]* Kazumasa Honda,[a] Yoshito Gotoh,[a] Akio Yoneyama,[b] Kazuhiro Ueda,[b] Atsushi Miyamoto,[c] Takeo Hondoh,[c] Akira Hori,[d] Duo Sun,[e] Ryo Ohmura,[e] Kazuyuki Hyodo[f] and Tohoru Takeda[g]

[a]Research Institute of Instrumentation Frontier, National Institute of Advanced Industrial Science and Technology, 1-1-1 Higashi, Tsukuba 305-8565, Japan, [b]Central Research Laboratory, Hitachi Ltd, 2520 Akanuma, Hatoyama 350-0395, Japan, [c]Institute of Low Temperature Science, Hokkaido University, N19 W8, Sapporo 060-0819, Japan, [d]Department of Civil and Environmental Engineering, Kitami Institute of Technology, 165 Koen-cho, Kitami 090-8507, Japan, [e]Department of Mechanical Engineering, Keio University, 3-14-1 Hiyoshi, Kohoku-ku, Yokohama 223-8522, Japan, [f]Institute of Materials Science, High Energy Accelerator Research Organization, 1-1 Oho, Tsukuba 305-0801, Japan, and [g]School of Allied Health Sciences, Kitasato University, 1-15-1 Kitasato, Sagamihara 228-8555, Japan. E-mail: s.takeya@aist.go.jp

Diffraction-enhanced imaging (DEI) is a phase-contrast X-ray imaging technique suitable for visualizing light-element materials. The method also enables observations of sample-containing regions with large density gradients. In this study a cryogenic imaging technique was developed for DEI-enabled measurements at low temperature from 193 K up to room temperature with a deviation of 1 K. Structure-II air hydrate and structure-I carbon dioxide (CO_2) hydrate were examined to assess the performance of this cryogenic DEI technique. It was shown that this DEI technique could image gas hydrate coexisting with ice and gas bubbles with a density resolution of about 0.01 g cm^{-3} and a wide dynamic density range of about 1.60 g cm^{-3}. In addition, this method may be a way to make temperature-dependent measurements of physical properties such as density.

Keywords: phase-contrast imaging; diffraction-enhanced imaging; X-ray interferometric imaging; non-destructive imaging; clathrate hydrate.

1. Introduction

Clathrate hydrates, so-called gas hydrates, are inclusion compounds consisting of a hydrogen-bonded crystal of water molecules with cages that contain gas molecules (Jeffrey, 1996; Sloan & Koh, 2008). Most gas hydrates are only stable at low temperature or high pressure. Natural gas hydrate, which includes methane (CH_4) as a major component, attracts attention as an unconventional natural resource (Kvenvolden, 2003). Also, air [a mixture of nitrogen (N_2), oxygen (O_2) and small amounts of other gases] hydrate in glacier ice in polar regions and carbon dioxide (CO_2) hydrate in deep ocean are known. However, it is not suitable to visualize weakly absorbing light-element materials such as gas hydrate co-existing with water or ice using conventional absorption-contrast X-ray imaging techniques (Jin *et al.*, 2004; Murshed *et al.*, 2008). Thus, X-ray absorption-contrast imaging requires an additive to visualize gas hydrates coexisting with water, to enhance the difference in density between the hydrate and water (Jin *et al.*, 2008; Kerkar *et al.*, 2009). Magnetic resonance imaging can identify gas hydrates coexisting with water (Moudrakovski *et al.*, 1999; Gao *et al.*, 2005), but it has not been applied to a system coexisting with ice.

Phase-contrast X-ray imaging (PCXI) uses a phase shift for image contrast. In the 'hard X-ray' region the phase-shift cross section for light elements is about 1000 times larger than that of absorption (Momose *et al.*, 1995). Several methods have been proposed for detecting these phase shifts. Among these, X-ray interferometric imaging (XII) (Bonse & Hart, 1965; Momose *et al.*, 1995) and diffraction-enhanced imaging (DEI) (Chapman *et al.*, 1997) have been mainly used for two- and three-dimensional observations of samples several centimetres in size. However, so far there have been few studies made at low or high temperature because of the difficulty in controlling the temperature of samples without interrupting measurements of the X-ray phase-shift. Thermal influence in PCXI is negligible because thermal drift of the asymmetric crystal and analyzer crystal for DEI or deformations of crystal wafers for XII reduce the sensitivity of PCXI.

We have shown that it is possible to visualize air hydrate in ice (Takeya *et al.*, 2006), THF hydrate in THF solution (Takeya *et al.*, 2007) and CH_4 hydrate coexisting with ice (Takeya *et al.*, 2011) using XII. The advantage of PCXI is more pronounced in elements with low atomic numbers, such as carbon and oxygen. While XII is suitable for detecting gradual phase shifts and absolute densities of materials with high density resolution ($\sim$0.001 g cm^{-3}) (Yoneyama *et al.*, 2008), it is limited by a sample outlining effect arising from a large phase shift caused by the difference in density between the sample and air. However, DEI allows a wider dynamic density range to be probed, and enables observation of samples containing regions with large density gradients (Yoneyama *et al.*, 2008). Thus, the density resolution of DEI is not as high as that of XII, but it may still be applicable to gas hydrate systems containing gas bubbles.

In this paper we report methods for observing gas hydrates using the DEI system equipped with a specially designed cryo-chamber. Our techniques allow non-destructive three-dimensional observations of various materials at low temperature. Also, our experimental results are valuable for assessing DEI because ice and gas hydrate crystals are among the lowest-density crystals. Moreover, developing the cryo-chamber, which can be used in both DEI and XII, may broaden the application range of PCXI.

2. Experimental methods

Phase-contrast X-ray images were obtained using monochromatic synchrotron X-rays at a vertical wiggler beamline (BL-14C) at the Photon Factory in Tsukuba, Japan. We monochromated the X-rays to 35 keV using a Si(220) double-crystal monochromator and enlarged the beam horizontally using an asymmetric Si(220) crystal with an asymmetric angle of 3.5°. For DEI, we irradiated the sample with an incident monochromatic X-ray beam enlarged horizontally by an asymmetric Si(220) crystal. The X-ray beam that passed through the sample was diffracted by a Si(220) analyzer crystal and then entered an X-ray imager (Fig. 1*a*) (Yoneyama *et al.*, 2007). We produced a phase map using two (*i.e.* 'T') images (DEIT) obtained by scanning the analyzer crystal at each position, giving a total measurement time of about 60 min. The DEI field of view was 25 mm × 35 mm with a spatial resolution of about 40 µm. To obtain three-dimensional phase-contrast X-ray computed tomography images we rotated the sample by 180° in 0.72° steps in a cryo-chamber.

We specially designed the cryo-chamber for PCXI experiments with synchrotron radiation at low temperature (see Fig. 1*b*). The sample chamber was made of aluminium with a size of 210 mm (width) × 165 mm (length) × 230 mm (height). The temperature of the cryo-chamber was controlled by blowing temperature-controlled dry N_2 gas supplied by a liquid N_2 container of 50 L, which can be done continuously for more than 12 h. The cryo-chamber was insulated by a vacuum layer, and the temperature outside was kept at room temperature. Thus, the cryo-chamber did not disturb the measurement of the X-ray phase shift using an asymmetric crystal and an analyzer crystal. An X-ray window made of aluminium foil with a thickness of 0.5 mm was put at each end of the sample chamber. The size of these windows was adjusted to 60 mm × 30 mm for XII measurements using a two-crystal X-ray interferometer (Yoneyama *et al.*, 2004) so that the object X-ray beam and the reference X-ray beam could pass through them. The windows were composed of a two-layer structure, and the layer was also vacuumed for insulation. The insulation prevented condensation from occurring on the windows owing to the difference between the room temperature and the low temperature in the chamber.

A copper cell consisting of two X-ray windows 25 mm × 35 mm in size was mounted inside the cryo-chamber (see Fig. 1*c*). These X-ray windows were also made of aluminium foil with a thickness of 0.5 mm. We attached two sheet heaters to the cell to control the temperature of the liquid that was introduced into it, and a thermocouple was attached to the middle of the cell to measure the liquid temperature. Accordingly, the liquid temperature was controlled with a

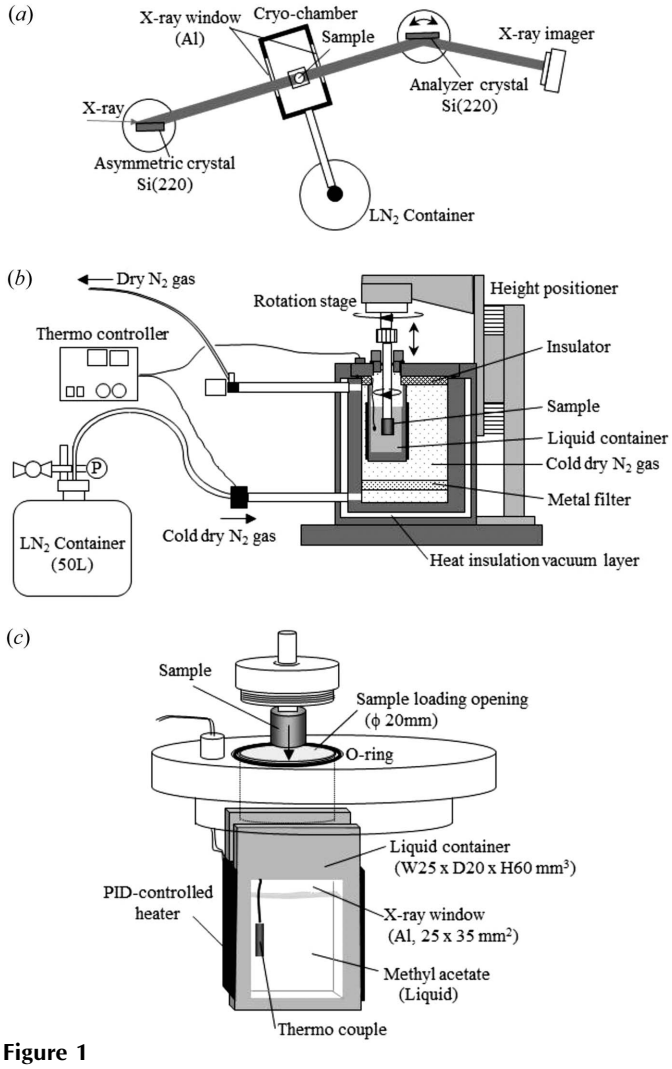

Figure 1
Schematic of the experimental set-up for cryogenic DEI measurement. (*a*) Top view including DEI optical system; (*b*) cryogenic system and sample positioning system; (*c*) method of loading sample into the liquid container.

deviation of 1 K. The sample was soaked in the temperature-controlled liquid. The liquid around the sample prevented undesirable outline contrasts from the outer surface of the sample, allowing internal observation. We selected methyl acetate (99.5%, Kishida Chemical Co.) as the liquid for this study because the density of methyl acetate is 0.928 g cm^{-3} at 298 K, which is close to that of hexagonal ice (0.917 g cm^{-3} at 273 K). Additionally, methyl acetate can be kept in a liquid state even at low temperature, since its melting point is 175 K. Note that the type of liquid material can be selected based on the density of the objective sample and the experimental temperature. We immersed the sample in pre-cooled liquid methyl acetate to avoid hydrate dissociation. For the density analysis we also measured a single crystal of hexagonal ice immersed in liquid methyl acetate at 193 K as an external standard of density. X-ray diffraction measurements have estimated the density of such a crystal to be 0.927 g cm^{-3} at 193 K (Röttger *et al.*, 1994).

3. Phase-contrast X-ray images

Herein we performed non-destructive imaging of gas hydrates coexisting with ice to test the performance of cryogenic DEI. For this purpose we examined air hydrate of structure II (*Fd*3*m*), which is the first gas hydrate visualized by XII, and carbon dioxide (CO_2) hydrate of structure I (*Pm*3*n*).

3.1. Air hydrate

Air hydrate is a clathrate hydrate containing air in its cage structures. Understanding air hydrates is essential for reconstructing climates over the last several hundred thousand years, because the gas concentration measurements that are mainly obtained from air hydrate in deep ice cores provide important information about paleo-atmospheres (Pauer *et al.*, 1995). In addition, it is known that air hydrate crystals are single crystals several hundreds of micrometres in diameter (Hondoh *et al.*, 1990; Takeya *et al.*, 2000), which enables us to estimate the density of the material. In the case of polycrystals, accurate density analysis requires the effect of grain boundaries and pore spaces to be taken into account. In this respect, observing air hydrate crystals within ice crystals is ideal for assessing cryogenic DEI.

Fig. 2 shows DEI images of ice cores drilled from Dome Fuji in Antarctica measured at 213 K. Fig. 2(*a*) shows that there are many particles in the ice sample drilled from 2175.8 m, which corresponds to the areas where the densities are higher than that of the surrounding ice (0.927 g cm^{-3} at 193 K). Although absolute densities of air hydrates are determined by cage occupancy, which depends on their formation conditions and paleo-atmospheres, XII shows that the density of air hydrates is 0.014 $\pm$ 0.003 g cm^{-3} higher than that of ice at 233 K (Takeya *et al.*, 2006). Therefore, air hydrate crystals were successfully visualized by DEI. Also, the imaging showed some gas bubbles ($\sim$0 g cm^{-3}) caused by dissociation from the air hydrates. It is reported that the density resolution of DEI is lower than that of XII, but that the density resolution of XII

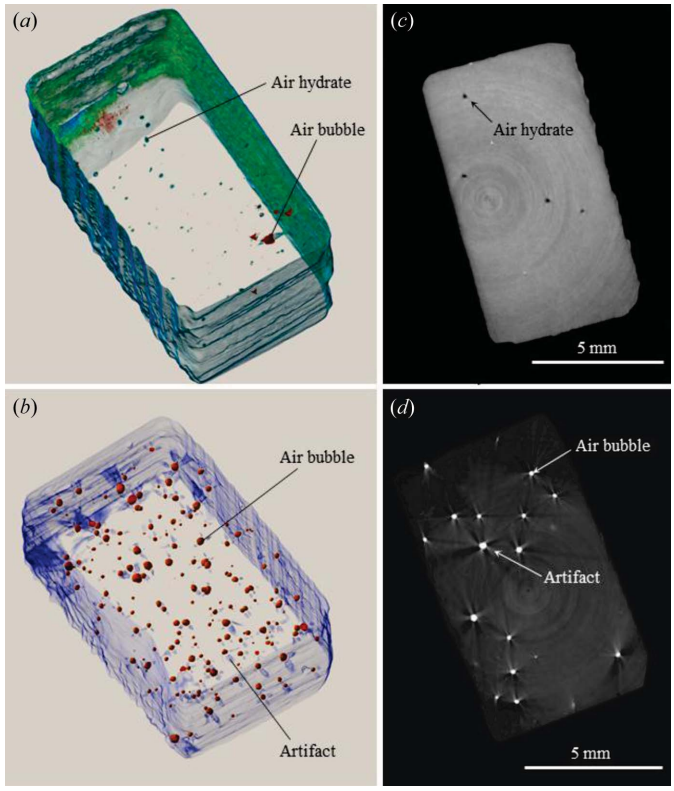

Figure 2
DEI images of ice core samples. These core samples showing three dimensions were drilled from depths of (*a*) 2175.8 m and (*b*) 575.8 m. The internal parts of the images were made transparent to show the inclusions more clearly. The cross sections in (*a*) and (*b*), which are cut through almost at the centre of each ice core, are shown in (*c*) and (*d*), respectively. Here, green regions in the images indicate areas where the densities are higher than that of the surrounding hexagonal ice, which corresponds to air hydrate. Also, red regions in the images indicate areas where the densities are lower than that of the surrounding hexagonal ice, which correspond to air bubbles.

and DEIT is comparable and higher than 0.01 g cm^{-3} in this energy region (35 keV). The cross-section image with slice thickness of 25 µm shown in Fig. 2(*c*) also reveals that air hydrate crystals can be clearly visualized. Therefore, our experimental result suggests that the cryogenic method we developed did not reduce the imaging sensitivity.

Fig. 2(*b*) shows that air bubbles that did not transform into air hydrates remained inside of the ice core at 575.8 m. Also, the cross-section image with slice thickness of 25 µm shown in Fig. 2(*d*) suggests that gas bubbles can be clearly visualized even though artifacts occurred around air bubbles owing to large density difference between the ice and air bubbles. Although the XII cannot visualize ice samples containing gas bubbles owing to the large density gradient, these results clearly show that the DEI allows visualization of both air hydrate and air bubbles in ice at one time. Accordingly, it was shown that the dynamic density range of the DEI method was at least from $\sim$0 to 0.95 g cm^{-3}.

3.2. CO_2 hydrate

CO_2 hydrate is one of the best understood gas hydrates in terms of structural, thermodynamic and other physical prop-

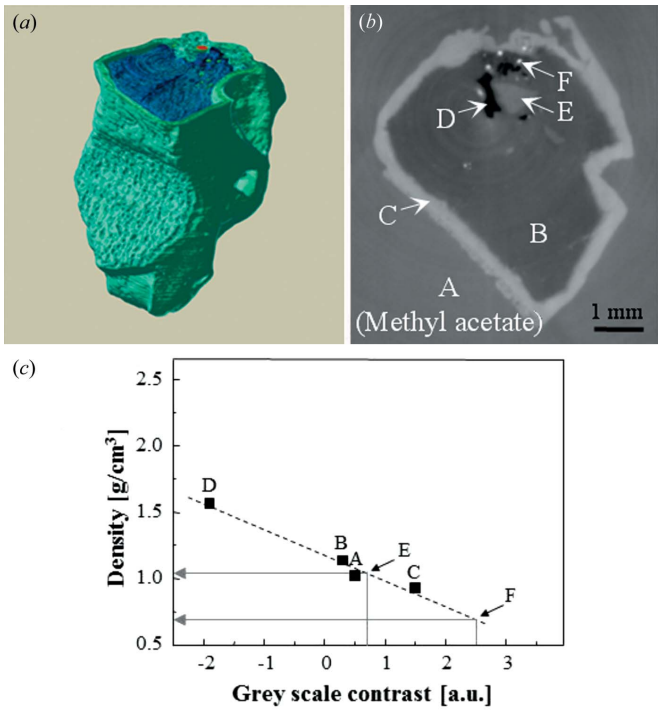

Figure 3
(*a*) Three-dimensional DEI image of a CO_2 hydrate. The blue regions indicate CO_2 hydrate and the light green regions indicate ice. Also, the red circle indicates an air bubble. (*b*) DEI image of the cross section of the hydrate sample. (*c*) Density of material as a function of the grey-scale level of the DEI image in (*b*). Here, the letters represent the grey-scale levels obtained in (*b*).

erties. CO_2 hydrate occurs as natural deposits in the solar system (Trainer *et al.*, 2010) as well as on earth (Sakai *et al.*, 1990). Recently, several researchers have conducted laboratory and field studies to produce hydrate from CO_2 waste or flue gas because hydrate is a potential means of controlling CO_2 build-up in the atmosphere by storing CO_2 (Englezos & Lee, 2005; Sun *et al.*, 2011).

We synthesized the CO_2 hydrate sample by mixing liquid water and CO_2 gas in a high-pressure vessel. Then we removed the formed hydrate sample at a temperature below 170 K after quenching the vessel by immersing it in liquid nitrogen. X-ray diffraction revealed that the CO_2 hydrate sample was a mixture of structure-I CO_2 hydrate and hexagonal ice as expected. Fig. 3(*a*) shows non-destructive images obtained of the CO_2 hydrate measured with DEI at 193 K (see supplementary movie[1]). The grey-scale level of this X-ray image is inversely proportional to the density of the sample. Thus it was shown that hexagonal ice exists on the surface of the CO_2 hydrate sample, which may have formed from excess water during the quenching process after the sample synthesis. Interestingly, the cross-sectional image of the CO_2 hydrate shows four different grey-scale levels except hexagonal ice. (see Fig. 3*b*). It was also revealed that this CO_2 hydrate sample had a distribution of microstructures in the bulk sample, which may be caused by the synthesis process.

[1] Supplementary data for this paper are available from the IUCr electronic archives (Reference: WA5029). Services for accessing these data are described at the back of the journal.

Here we attempt a quantitative density analysis of the CO_2 hydrate sample. The grey-scale level of liquid methyl acetate [represented by A in Fig. 3(*b*)] measured with DEI was 0.5, and another DEI measurement of ice at 193 K showed that the density of liquid methyl acetate ($\sim$1.1 g cm^{-3}) was higher than that of hexagonal ice. The density of CO_2 hydrate at 193 K is known to be 1.136 g cm^{-3} (Udachin *et al.*, 2001) and that of ice is 0.927 g cm^{-3} (Röttger *et al.*, 1994). Thus, the regions with a grey-scale level of 0.3 [represented by B in Fig. 3(*b*)] correspond to CO_2 hydrate (1.136 g cm^{-3}), and those with 1.5 [represented by C in Fig. 3(*b*)] correspond to ice (0.927 g cm^{-3}) within the instrumental special resolution. At the same time it is estimated that the three unknown regions with grey-scale levels of -1.9, 0.7 and 2.5 correspond to densities of 1.5, 1.1 and 0.8 g cm^{-3}, respectively [represented by D, E and F, respectively, in Fig. 3(*c*)]. Because the density of solid CO_2, so-called dry ice, is 1.565 g cm^{-3} at 193 K, the regions with a grey-scale level of -1.9 correspond to solid CO_2, where unreacted CO_2 may transform into its solid phase owing to quenching during its synthesis. This is our preliminary result on CO_2 hydrate, and it remains unclear what the regions with intermediate grey-scale levels are. However, it is speculated that the higher-density region [represented by E in Fig. 3(*b*)] may correspond to a mixture of solid phases (CO_2 hydrate, ice and dry ice) and the lower-density region [represented by F in Fig. 3(*b*)] may correspond to a mixture of these solid phases and gas phases (air or CO_2 gas) according to powder X-ray diffraction results. While further study is necessary to answer the question, we suggest that DEIT is useful not only for non-destructive observation of gas hydrates but also for quantitative density analysis by means of X-ray images. Although cryogenic XII cannot visualize CO_2 hydrate samples coexisting with dry ice and gas bubbles owing to the large density gradient, we showed here that cryogenic DEI allows measurements over a wide density range from $\sim$0.00 to 1.60 g cm^{-3} within liquid methyl acetate at one time.

Finally, it should be noted that isothermal measurements are necessary especially for high-density resolution observations. For instance, a temperature deviation of 5 K corresponds to a density deviation of about 0.001 g cm^{-3} for CO_2 hydrate, while an XII density resolution is about 0.001 g cm^{-3}. In this respect the controlled performance of the cryochamber within a temperature deviation of several K enables high-density resolution measurements. In principle, temperature-controlled measurements at temperatures higher than room temperature are equivalent to that performed in this study. We are currently trying to apply our method not only to medical or biological imaging but also to imaging of materials or devices such as polymer electrolyte fuel cells. These samples, composed of light element such as carbon, nitrogen and oxygen, are good candidates for DEI measurements under higher-temperature conditions ($\sim$400 K).

4. Summary

DEI is a PCXI technique suitable for visualizing light-element materials. In this study we developed a chamber for PCXI

experiments using synchrotron radiation at low temperature. The temperature of the cryo-chamber was controlled by blowing temperature-controlled dry N_2 gas supplied by liquid N_2. The temperature range was from 193 K to room temperature with a deviation of 1 K, and could be controlled continuously for more than 12 h. The chamber is also applicable to XII owing to a large X-ray window of 60 mm × 30 mm. The results obtained for air hydrate and CO_2 hydrate show that our DEI technique is suitable for imaging gas hydrate coexisting with ice and gas bubbles with a density resolution of about 0.01 g cm^{-3} and a dynamic density range of about 1.60 g cm^{-3}. We also found four different crystal phases or microstructures within the CO_2 bulk sample other than hexagonal ice: CO_2 hydrate, solid CO_2 and two unknown phases. These results suggest that DEIT is useful not only for non-destructive observation of gas hydrates but also for quantitative density analysis by means of X-ray images.

This study was carried out under Proposals Nos. 2010G170 and 2009S2-006, and was approved by the High Energy Accelerator Research Organization. We thank all the participants of the Japan Antarctic Research Expedition (JARE) for the drilling, field work and ice sampling. Part of this study was supported by JSPS KAKENHI 40357421.

References

Bonse, U. & Hart, M. (1965). *Appl. Phys. Lett.* **6**, 155–156.
Chapman, D., Thomlinson, W., Johnston, R. E., Washburn, D., Pisano, E., Gmür, N., Zhong, Z., Menk, R., Arfelli, F. & Sayers, D. (1997). *Phys. Med. Biol.* **42**, 2015–2025.
Englezos, P. & Lee, J. D. (2005). *Kor. J. Chem. Eng.* **22**, 671–681.
Gao, S., House, W. & Chapman, W. G. (2005). *J. Phys. Chem. B*, **109**, 19090–19093.
Hondoh, T., Anzai, H., Goto, A., Mae, S., Higashi, A. & Langway Jr, C. C. (1990). *J. Inclusion Phenom. Mol. Recognit. Chem.* **8**, 17.
Jeffrey, G. A. (1996). *Comprehensive Supramoloecular Chemistry*, Vol. 6, edited by J. L. Atwood, J. E. D. Davies, D. D. MacNicol and F. Vogtle. Oxford: Pergamon/Elsevier.
Jin, S., Takeya, S., Hayashi, J., Nagao, J., Kamata, Y., Ebinuma, T. & Narita, H. (2004). *Jpn. J. Appl. Phys.* **43**, 5673–5675.
Jin, Y., Nagao, J., Hayashi, J., Shimada, W., Ebinuma, T. & Narita, H. (2008). *J. Phys. Chem. C*, **112**, 17253–17256.
Kerkar, P., Jones, K. W., Kleinberg, R., Lindquist, W. B., Tomov, S., Feng, H. & Mahajan, D. (2009). *Appl. Phys. Lett.* **95**, 024102.
Kvenvolden, K. A. (2003). *Natural Gas Hydrate in Oceanic and Permafrost Environments*, edited by M. D. Max. Berlin: Springer Verlag.
Momose, A., Takeda, T. & Itai, Y. (1995). *Rev. Sci. Instrum.* **66**, 1434–1436.
Moudrakovski, I. L., Ratcliffe, C. I., McLaurin, G. E., Simard, B. & Ripmeester, J. A. (1999). *J. Phys. Chem. A*, **103**, 4969–4972.
Murshed, M. M., Klapp, S. A., Enzmann, F., Szeder, T., Huthwelker, T., Stampanoni, M., Marone, F., Hintermuller, C., Bohrmann, G., Kuhs, W. F. & Kersten, M. (2008). *Geophys. Res. Lett.* **35**, L23612.
Pauer, F., Kipfstuhl, J. & Kuhs, W. F. (1995). *Geophys. Res. Lett.* **28**, 969–971.
Röttger, K., Endriss, A., Ihringer, J., Doyle, S. & Kuhs, W. F. (1994). *Acta Cryst.* B**50**, 644–648.
Sakai, H., Gamo, T., Kim, E. S., Tsutsumi, M., Tanaka, T., Ishibashi, J., Wakita, H., Yamano, M. & Oomori, T. (1990). *Science*, **248**, 1093–1096.
Sloan, E. D. & Koh, C. A. (2008). *Clathrate Hydrates of Natural Gases*, 3rd ed. Boca Raton: CRC/Taylor Francis.
Sun, D., Shimono, Y., Takeya, S. & Ohmura, R. (2011). *Ind. Eng. Chem. Res.* **50**, 13854–13858.
Takeya, S., Honda, K., Kawamura, T., Yamamoto, Y., Yoneyama, A., Hirai, Y., Hyodo, K. & Takeda, T. (2007). *Appl. Phys. Lett.* **90**, 081920.
Takeya, S., Honda, K., Yoneyama, A., Hirai, Y., Okuyama, J., Hondoh, T., Hyodo, K. & Takeda, T. (2006). *Rev. Sci. Instrum.* **77**, 053705.
Takeya, S., Nagaya, H., Matsuyama, T., Hondoh, T. & Lipenkov, V. Ya. (2000). *J. Phys. Chem. B*, **104**, 668–670.
Takeya, S., Yoneyama, A., Ueda, K., Hyodo, K., Takeda, T., Mimachi, H., Takahashi, M., Iwasaki, T., Sano, K., Yamawaki, H. & Gotoh, Y. (2011). *J. Phys. Chem. C*, **115**, 16193–16199.
Trainer, M. G., Tolbert, M. A., McKay, C. P. & Toon, O. B. (2010). *Icarus*, **206**, 707–715.
Udachin, K. A., Ratcliffe, C. I. & Ripmeester, J. A. (2001). *J. Phys. Chem. B*, **105**, 4200–4204.
Yoneyama, A., Jin, W., Hyodo, K. & Takeda, T. (2008). *Med. Phys.* **35**, 4724–4734.
Yoneyama, A., Takeda, T., Tsuchiya, Y., Wu, J., Lwin, T. T. & Hyodo, K. (2004). *AIP Conf. Proc.* **705**, 1299–1302.
Yoneyama, A., Takeda, T., Wu, J., Lwin, T. T., Hyodo, K. & Hirai, Y. (2007). *Jpn. J. Appl. Phys.* **46**, 1205–1207.